Int. J. Electrochem. Sci., 11 **(2016)** 5973 – 5982, doi: 10.20964/2016.07.84

International Journal of ELECTROCHEMICAL SCIENCE
www.electrochemsci.org

Formation and Fluctuation-Induced Conductivity of $(Tl_{1-x}Bi_x)Sr_2CaCu_2O_{7-\delta}$ (x = 0.1- 0.7) Superconductor

S.S.O Farhat, R. Abd-Shukor[*]

School of Applied Physics, Universiti Kebangsaan Malaysia, 43600 Bangi, Selangor, Malaysia
[*]E-mail: ras@ukm.edu.my

Received: 26 March 2016 / *Accepted:* 4 May 2016 / *Published:* 4 June 2016

The $(Tl_{1-x}Bi_x)Sr_2CaCu_2O_{7-\delta}$ (x = 0.1, 0.2, 0.3, 0.4, 0.5,and 0.7) samples were prepared by the solid-state reaction method. The samples were studied by powder X-ray diffraction method, electrical resistance measurements and energy dispersive X-ray analysis (EDX). All samples showed a dominant Tl-1212 phase with volume fraction approximately 85%. The Aslamazov-Larkin (AL) theory was used to analyze the excess conductivity. The dimension of fluctuation induced conductivity λ was also determined using the AL theory. The coherence length $\xi_c(0)$, Josephson coupling J, and anisotropy $\gamma = (\xi_{ab}(0)/\xi_c(0))$ of the samples was calculated using the Lawrence-Donaich (LD) theory. Substituting Bi into $(Tl_{1-x}Bi_x)Sr_2CaCu_2O_{7-\delta}$ (Tl-1212) caused an initial increase in the zero-resistance-temperature ($T_{c\ zero}$). The samples with x = 0.3 and 0.4 showed the highest $T_{c\ onset}$ (101 K). Excess conductivity analyses showed that Bi substitution induced 2D-to-3D conductivity transition with the highest transition temperature, T_{2D-3D} observed at x = 0.3. The shortest coherence length, $\xi_c(0)$ and lowest interplanar coupling, J was observed in the x = 0.7 which is in the under-doped state.

Keywords: Tl-1212 type phase; coherence length; anisotropy; superconductor

1. INTRODUCTION

The $TlSr_2CaCu_2O_7$ (Tl-1212) phase with average Cu valence of + 2.25 exhibits the highest superconducting transition similar to $YBa_2Cu_3O_7$ (Y-123) [1]. The Tl-1212 phase is not easy to synthesize in pure form [2, 3]. Substitution of elements with higher valence in the $TlSr_2CaCu_2O_7$ phase may reduce the formal valence of Cu to the optimal value. Such substitution can also stabilize the 1212 phase and improve its superconducting characteristics [4–9]. Substitution of rare-earth elements (R) into the Sr^{2+} site [1, 5, 10-12] and Ca^{2+} site [1, 10-12] facilitates the formation of the Tl-1212 phase. $TlSr_2(Ca,R)Cu_2O_7$ with transition temperature (T_c) of 90 K have been reported [13,14]. Partial replacement of Tl^{3+} with Bi [15,16], Pb [16,18] or Cr [17, 19] facilitates the Tl-1212 phase formation.

High temperature superconductors (HTSCs) including Tl-1212 show large anisotropy in the superconducting and normal state. This large anisotropy promotes fluctuation in the order parameter owing to the short coherence length along the *c*-axis, $\xi_c(0)$. The linear resistivity curve deviates downward at the critical temperature as a result of enhanced conductivity due to the superconducting fluctuations [20]. The Aslamazov-Larkin (AL) and the Lawrence-Doniach (LD) model can be used to study the excess conductivity in the HTSC. Excess conductivity can be given by [21]:

$$1/\Delta\rho = 1/\rho_{\text{measured}} - 1/\rho_{\text{background}} \qquad (1)$$

where ρ is the resistivity. Excess conductivity can written as [22]:

$$\Delta\sigma/\sigma_o = A\,\varepsilon^{-\lambda} \qquad (2)$$

where σ_o is the conductivity at 300 K, ε is the reduced temperature given by the relation [23]:

$$\varepsilon = \ln(T/T^p_c) / T^p_c = (T - T^p_c) / T^p_c\,. \qquad (3)$$

T^p_c is the temperature of the peak obtained from the derivative of resistivity versus temperature curve, *A* is a constant. The dimensionality of the conduction D is related to the critical exponent λ where $\lambda = 2 - D/2$. For 1D region, λ = 1.5, for 2D, λ = 1.0, and for 3D, λ = 0.5. The slope of $\ln(\Delta\sigma/\sigma_o)$ versus $\ln(\varepsilon)$ plot can be used to calculated λ. Elemental substitutions also result in changes in T_{2D-3D} and coherence length [24]. For Tl-1212, this enhancement leads to enhancement of the superconducting properties and longer $\xi_c(0)$ as a result of the reduction in γ and increase in *J* [24]. For a polycrystalline sample, T_{2D-3D} and $\xi_c(0)$ can be determined by using the Lawrence-Doniach model [23]:

$$T_{2D-3D} = T_c\,[1 + (2\,\xi_c(0)/d)^2] \qquad (4)$$

In this work, $d = 3.18$ Å is the distance between superconducting layers of Tl-1212 [23]. The Lawrence-Doniach model also introduced the concept of interlayer coupling, *J* based on Josephson coupling as a result of $\xi_c(0)$ interaction with superconducting layers. The relation between $\xi_c(0)$ and interlayer coupling, *J* is given by [25]:

$$J = [2\,\xi_c(0)]^2/d^2 \qquad (5)$$

The anisotropy, γ of layered superconducting systems is expressed by [26]:

$$\gamma = \xi_{ab}(0) / \xi_c(0) \qquad (6)$$

Generally, $\xi_{ab}(0)$ is the *ab*-coherence length which is between 10 and 20 Å for oxide high-temperature superconductors [23].

There have been several reports on the effect of Cr on the superconductivity and formation of the Tl-1212 phase [27]. The (Cu, Tl)-based [28-31] revealed a cross over from 2D to 3D fluctuation behavior with decreasing temperature. $Tl_{1-x}Cu_xSr_{1.2}Yb_{0.8}CaCu_2O_{7-d}$ [32] and $Tl_{0.5}Pb_{0.5}Sr_{2-x}Yb_xCaCu_2O_{7-d}$ [28] showed strong influence of the substitutions on fluctuation behavior with transition from 2D to 3D. Interestingly, $Tl_{0.8}Hg_{0.2}Ba_2\,Ca_{2-x}R_xCu_3O_{9-d}$ (R = Sm and Yb) revealed the transitions from 1D to 2D and 2D to 3D as the temperature was lowered [33].

Substitution of multivalent ions such as chromium results in a higher T_c than a single valent ions such as most of rare-earth elements. Bi is another element with multivalent ion. Bi_2O_3 has been used in various studies including ionic conductivity studies and glass system [34, 35]. It is interesting to investigate the effect of multivalent bismuth (ionic radius of $Bi^{3+} \approx 1.13$ Å) at the Tl site (Tl^{3+} ionic radius ≈1.03 Å) in the Tl-1212 superconductor.

I n this paper, we report the effects of Bi substitution at the Tl site in $(Tl_{1-x}Bi_x)Sr_2CaCu_2O_{7-\delta}$ (x = 0.1 - 0.7) superconductors. Results of electrical resistance (dc) measurements using the four-point-probe method and powder X-ray diffraction are presented. The Aslamazov-Larkin (AL) theory was

employed as a framework to determine the dimension of fluctuation induced conductivity, λ. $\xi_c(0)$, J and γ of was calculated using the Lawrence-Donaich (LD) theory.

2. EXPERIMENTAL DETAILS

Samples with nominal starting composition $(Tl_{1-x}Bi_x)Sr_2CaCu_2O_{7-\delta}$ (x = 0.1, 0.2, 0.3, 0.4, 0.5 and 0.7) were prepared using the solid-state reaction method. High purity (≥ 99.99 %) SrO, CaO and CuO were mixed in appropriate amounts and ground before being calcined at 900 ºC for over 48 h with several intermittent grindings. Tl_2O_3 and Bi_2O_3 with appropriate amounts were added to the precursor and completely mixed. The powders were then pressed into pellets with diameter 13 mm and 2 mm thickness. In order to compensate for the thallium loss during heating, excess 10 % Tl_2O_3 was added. The pellets were heated at 1000 ºC for 4 min in flowing O_2 followed by natural cooling of the furnace.

The four-point probe method was used to measure the dc electrical resistance. Silver paste was used electrical contact. The low temperature measurements were performed in a CTI Cryogenics Closed Cycle Refrigerator Model 22 and Lake Shore Temperature Controller Model 340. $T_{c\ zero}$ is defined as the temperature where the electrical resistance becomes zero and $T_{c\ onset}$ is defined as the temperature where the resistance begins to drop sharply. The powder X-ray diffraction method using a Bruker model D8 Advance diffractometer with CuK_α source was used to determine the phase of the samples. At least 15 diffraction peaks were used to calculate the lattice parameters. The 1212:1201 volume fraction was calculated from the diffraction intensities of the respective phase using [23]:

$$\mathrm{Tl}-1212(\%) = \frac{\sum I_{1212}}{\sum I_{1212} + \sum I_{1201}} \times 100\% \qquad (5)$$

$$\mathrm{Tl}-1201(\%) = \frac{\sum I_{1201}}{\sum I_{1212} + \sum I_{1201}} \times 100\% \qquad (6)$$

where I is the peak intensity of the phases.

The elemental composition of the sample with x = 0.3 was determined using a Philips energy dispersive X-ray analyzer (EDX) model PV99.

3. RESULTS AND DISCUSSION

X-ray powder diffraction patterns for $(Tl_{1-x}Bi_x)Sr_2CaCu_2O_{7-\delta}$ (x = 0.1, 0.2, 0.3, 0.4, 0.5 and 0.7) are shown in Figure 1. The patterns indicated a single Tl-1212 phase with tetragonal unit cell (space group, P4/mmm) was dominant with few weak diffraction lines of Tl-1201, and an unknown phase. The x = 0.4 and 0.7 showed the highest Tl-1212 volume fraction (86%). Table 1 shows the values of $T_{c\ onset}$, $T_{c\ zero}$, resistivity (at 300 K), 1212:1201 volume fraction and 1212 lattice parameters for $(Tl_{1-x}Bi_x)Sr_2CaCu_2O_{7-\delta}$.

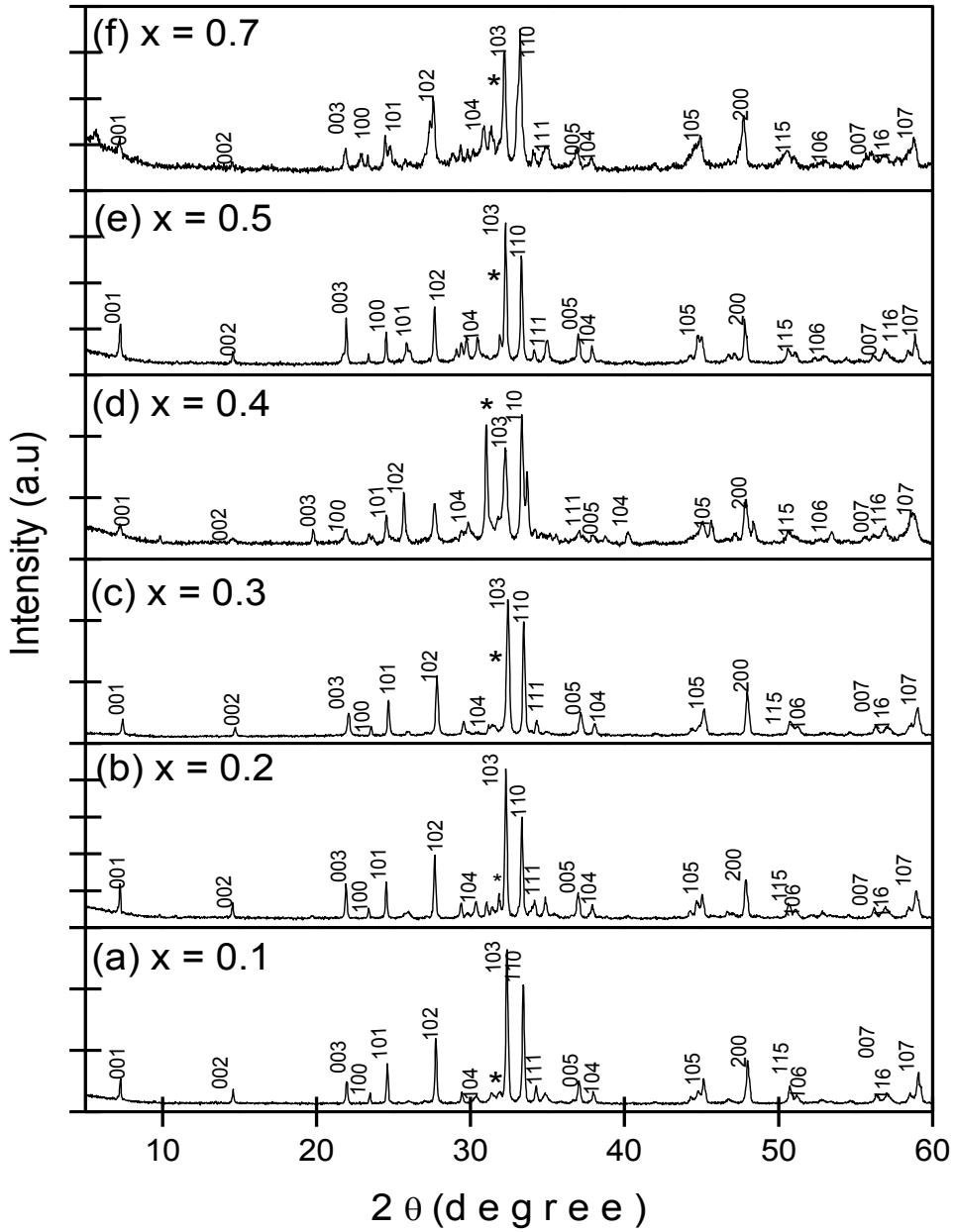

Figure 1. Powder X-ray diffraction patterns for $(Tl_{1-x}Bi_x)Sr_2CaCu_2O_{7-\delta}$ (x = 0.1, 0.2 0.15, 0.4, 0.5 and 0.7) samples showing major Tl-1212 phase. The 1201 phase is indicated by (*)

Table 1. $T_{c\ onset}$, $T_{c\ zero}$, lattice parameters, T^{ρ}_{c}, room temperature resistivity (ρ_{297}), α , β, $T_{2D\text{-}3D}$, λ_{2D}, λ_{3D}, $\xi_c(0)$, J and γ for $(Tl_{1-x}Bi_x)Sr_2CaCu_2O_{7-\delta}$ (x = 0.1, 0.2, 0.3, 0.4, 0.5 and 0.7) samples

x	0.1	0.2	0.3	0.4	0.5	0.7
$T_{c\ onset}$ (K)	81	87	101	101	94	85
$T_{c\ zero}$ (K)	44	77	87	87	82	52
1212:1201 volume fraction (vol. %)	84:16	83:17	83:17	86:14	83:17	86:14

Tl-1212 lattice parameter						
a (Å) ± 0.003	3.784	3.793	3.784	3.783	3.793	3.783
c (Å) ± 0.005	12.118	12.128	12.119	12.066	12.120	12.066
T^{ρ}_{c} (K)	48	79	88	89	84	60
ρ_{297} (mΩcm)	1.28	1.67	3.38	4.69	4.29	7.67
$\alpha = \rho_n$(0 K)(mΩcm)	0.16	0.20	1.20	1.40	2. 40	0.20
$\beta = d\rho/dT \times 10^{-3}$ (mΩcm)/K	3.35	4.29	6.89	5.13	6.22	1.35
T_{2D-3D} (K)	50	125	149	140	140	109
λ_{2D}	1.147	0.931	1.133	1.233	1.020	0.888
$\boldsymbol{\lambda}_{3D}$	0.499	0.533	0.482	0.477	0.454	0.428
γ	10.172	9.516	9.123	9.944	8.990	11.834
J	0.382	0.436	0.475	0.400	0.489	0.282
ξ_c(0) Å	0.983	1.050	1.096	1.005	1.112	0.845

Table 2. Elemental quantitative analysis of $(Tl_{1-x}Bi_x)Sr_2CaCu_2O_{7-\delta}$ superconductor for x = 0.3 superconductor as presented in EDX spectrum shown in Figure 5

x	Element	O K	Ca K	Cu L	Sr L	Tl M	Bi M	Total
0.3	Weight%	13.29	4.97	17.59	28.12	23.64	12.39	100
	Error%	0.65	0.38	0.79	1.05	1.38	1.55	
	Atomic%	48.10	7.18	16.02	18.57	6.69	3.43	

Figure 2 shows $T_{c\ onset}$ and $T_{c\ zero}$ versus Bi content. The normalized resistance as a function of temperature for the $(Tl_{1-x}Bi_x)Sr_2CaCu_2O_{7-\delta}$ samples for x = 0.1, 0.2, 0.3 0.4, 0.5 and 0.7 are shown in Figure 3. All samples displayed metallic normal-state behavior above $T_{c\ onset}$. The highest $T_{c\ onset}$ (101 K) and $T_{c\ zero}$ (87 K) was observed for x = 0.3 and 0.4. $T_{c\ zero}$ in the Bi substituted samples which are lower than $T_{c\ zero}$ of the Cr substituted samples [36, 37].

The normal state electrical resistivity was fitted to $\rho = \alpha + \beta T$ for x = 0.1–0.7 (Figure 3) where α is the intercept and β the slope of the resistivity [13]. The deviation from linearity of the resistivity curve is due to excess conductivity as the Cooper pair began to form. The temperature dependence of the derivative of the resistivity is shown in the insets of Figure 3. The peak temperature (T^{ρ}_{c}) from the inset was used to calculate the reduced temperature (ε). A single peak at T_c, indicating a superconducting transition within the grains was observed in all samples. The values of $T^{\rho}_{c,}$ the room temperature resistivity (ρ_{297}), α and β are shown in Table 1.

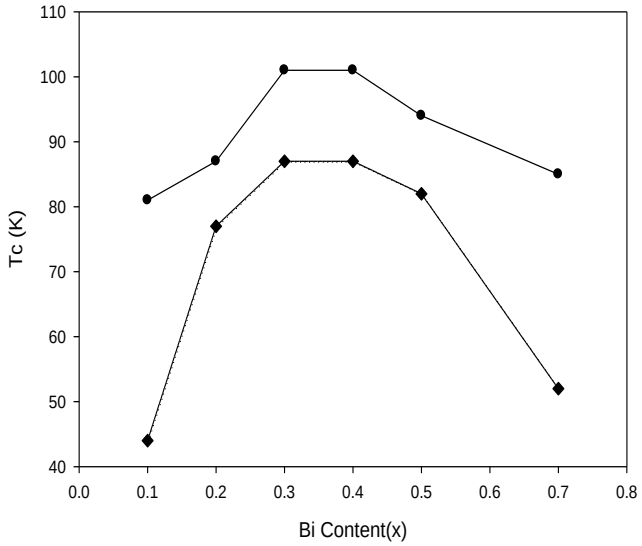

Figure 2. $T_{c\ onset}$ (●) and $T_{c\ zero}$ (♦) as a function of x for $(Tl_{1-x}Bi_x)Sr_2CaCu_2O_{7-\delta}$

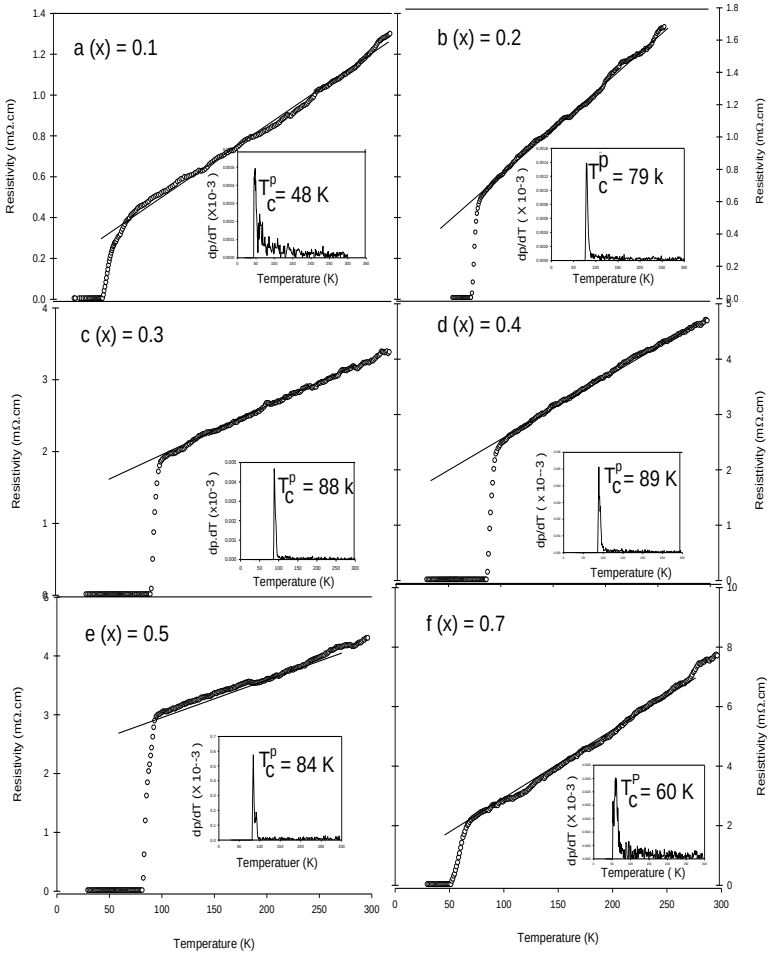

Figure 3. Electrical resistivity of $(Tl_{1-x}Bi_x)Sr_2CaCu_2O_{7-\delta}$ (x = 0.1, 0.2, 0.3, 0.4, 0. 5 and 0.7) samples. Insets show plots of dρ/dT versus temperature. The linear fit curves show the background normal state resistivity projection

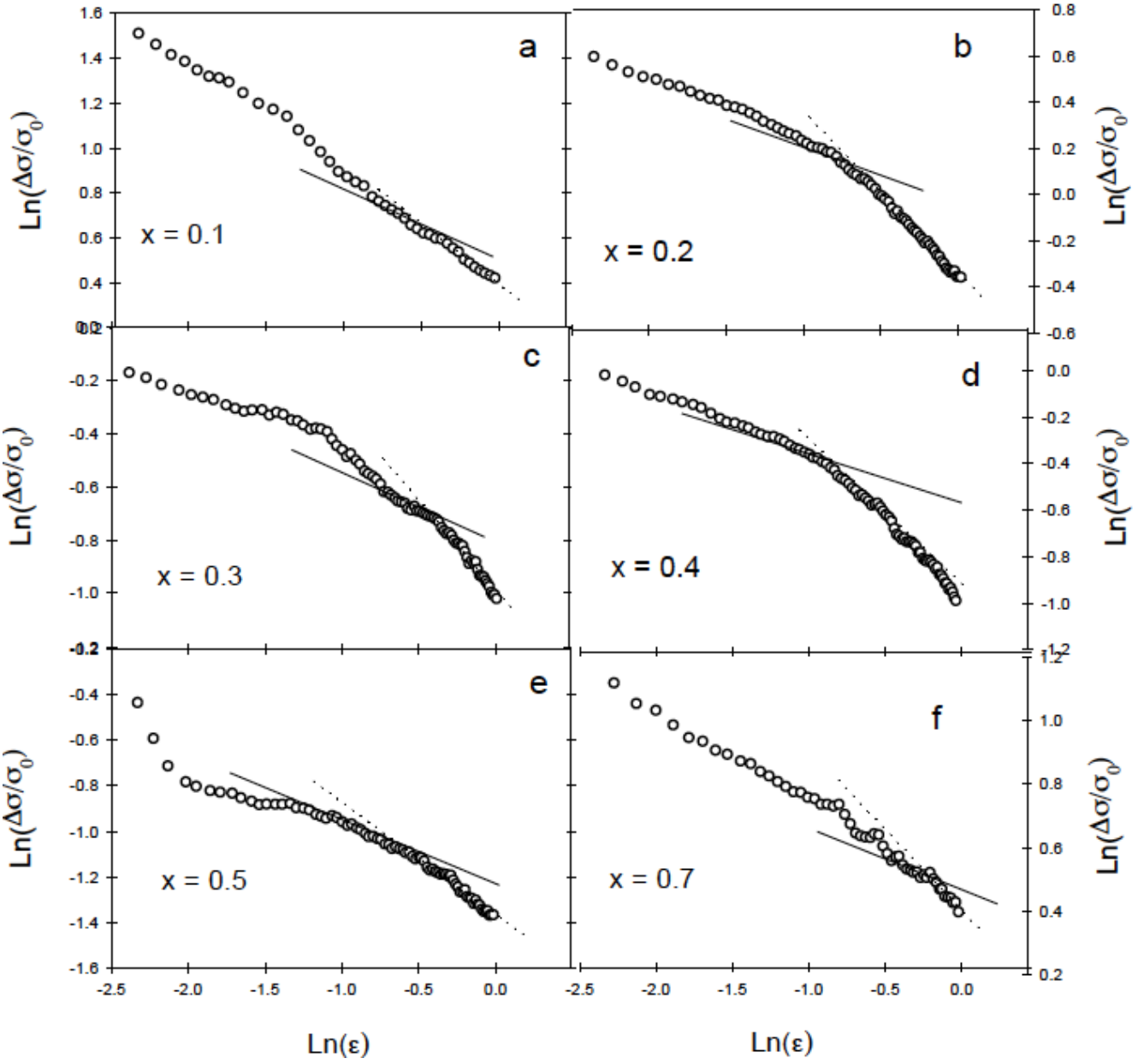

Figure 4. Plot of ln(Δσ/σo) versus ln(ε) of $(Tl_{1-x}Bi_x)Sr_2CaCu_2O_{7-\delta}$ (x = 0.1, 0.2, 0.3, 0.4, 0.55 and 0.7) samples. The solid line represents the 2-D and dotted line 3-D theoretical slope

Excess conductivity (Δσ) was indicated by the deviation of the resistivity $\rho(T)$ from the linear background resistivity curve. A graph of $\ln(\Delta\sigma/\sigma_o)$ versus ln(ε) was plotted (Figure 4) to compare the experimental data with the theoretical expression for fluctuation conductivity. This figure shows the fluctuation conductivity for all samples covering the mean field regime: $-3 < ln(\varepsilon) < 1$. As the temperature was decreased a transition from 2D- to 3D behavior was observed. The calculated values for $T_{2D\text{-}3D}$, $\xi_c(0)$, J and γ for the $(Tl_{1-x}Bi_x)Sr_2CaCu_2O_{7-\delta}$ samples are shown in Table 1. The shortest $\xi_c(0)$ within the series was 0.845 Å at $x = 0.7$. This sample also showed the lowest J value (0.282) and the highest anisotropy (γ) (11.834).

Figure 5 shows the EDX spectrum of $(Tl_{1-x}Bi_x)Sr_2CaCu_2O_{7-\delta}$ superconductor for x = 0.3. Table 2 shows the elemental composition of $(Tl_{1-x}Bi_x)Sr_2CaCu_2O_{7-\delta}$ superconductor for x = 0.3. The energy dispersive X-ray (EDX) analysis shows the presence of elements approximately according to composition of host superconducting matrix Tl-1212 with slight modification due to the presence of the 1201 phase and the uncertainty in determining the oxygen content by using the EDX method.

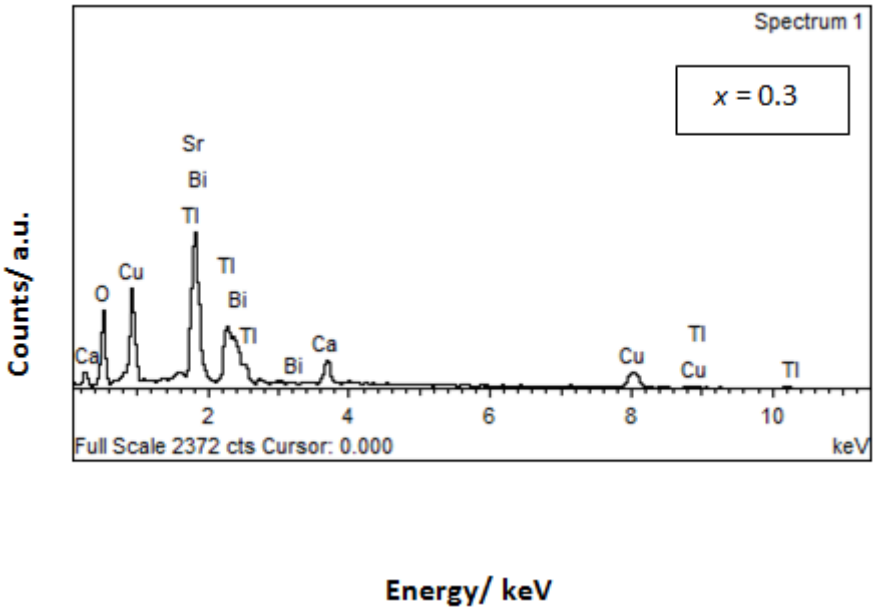

Figure 5. EDX spectrum of $(Tl_{1-x}Bi_x)Sr_2CaCu_2O_{7-\delta}$ superconductor for x = 0.3

The x = 0.3 and 0.4 samples showed the highest superconducting transition temperature. The decrease in the coherence length along the *c*-axis promotes an increase in anisotropy (γ) which possibly explains the superconducting behavior when $T_{c\ onset}$ exceeds 81 K. The average slope β increased from 3.35×10^{-3} to 6.89×10^{-3} (mΩ-cm)/K as x increased from 0.1 to 0.3 due to the change in carrier concentration when Bi-content was increased. The 2D- to 3D transitions in the normal state were induced by the partial substitution of Bi into Tl sites. Excess conductivity analyses revealed the dependence of $\xi_c(0)$ on the amount of Bi substitution in the $(Tl_{1-x}Bi_x)Sr_2CaCu_2O_{7-\delta}$. The highest $T_{2D–3D}$ was shown by the x = 0.3 and 0.4 samples.

Our results showed that lower anisotropy, longer coherence length $\xi(0)$ and higher T_{2D-3D} led to higher transition temperature T_c as shown by the x = 0.3, 0.4 and 0.5 samples. $(Tl_{0.5}Pb_{0.5})(Sr_{1.8}Yb_{0.2})(Ca_{1-y}Mg_y)Cu_2O_{7-d}$ samples also show the highest T_c for samples with the highest T_{2D-3D} [23]. $Cu_{0.5}Tl_{0.5}Ba_2(Ca_{2-y}Mg_y)(Cu_{0.5}Zn_{2.5})O_{10-d}$ also show a similar correlation between T_c and T_{2D-3D} [25]. A higher volume fraction of Tl-1212 phase did not show higher T_c, as shown by the x = 0.7 sample which is in the under-doped state. Hence, this work showed that T_{2D-3D} is important in determining the superconducting transition temperature.

4. CONCLUSION

This work showed that Bi was effective for the formation of the Tl-1212 phase. Excess conductivity analyses of $(Tl_{1-x}Bi_x)Sr_2CaCu_2O_{7-\delta}$ indicated that 2D to 3D transition in the normal state could be induced by partial substitution of Bi into Tl site. The x = 0.7 sample showed the lowest J (0.845) value and the highest anisotropy (γ) (11.834). These results indicated that Bi substitution modified J and the anisotropy of the samples. Bi substitution caused changes in T_{2D-3D} with the highest transition observed at x = 0.3.

ACKNOWLEDGEMENTS
This Ministry of Higher Education of Malaysia has supported this work under grant no.: FRGS/2/2013/SG02/UKM/01/1. Universiti Kebangsaan Malaysia also supported this work under grant no.: UKM-AP-2015-006.

References

1. S. Nakajima, M. Kikuchi, Y. Syono, N. Kobayashi and Y. Muto, *Physica* C 168 (1990) 57.
2. S. Maysuda, S. Takeuchi, A. Soeta, T. Suzuki, K. Alihara and T. Kamo, *Jpn. J. Appl. Phys*., 27 (1988) 2062.
3. T. Doi, K. Usami and T. Kamo, , *Jpn. J. Appl. Phys*. 29 (1990) L57.
4. Z. Y. Chen, Z. Z. Sheng, Y. Q. Tsang, Y. F. Li and D. O. Pederson, *Solid State Commun*., 83 (1992) 895.
5. W. H. Lee and B. C. Huang, *Physica* C 289 (1997)114.
6. R. S. Liu, Y. T. Huang, W. H. Lee, S. F. Fu and P. T. Wu, *Physica* C 156 (1988) 791.
7. R. S. Liu, W. Zhou, R. Janes and P. P. Edwards, *Solid State Commun, Solid State Science* 76 (1990) 1261.
8. A. K. Ganguli, K. S. Nanjundaswamy and C. N. R. Rao, *Physica* C 156 (1988) 788.
9. Y. Xin, Y. F. Li, D. Ford, D. O. Pederson and Z. Z. Sheng, *Jpn. J. Appl. Phys*., 30 (1991) 1549.
10. J. M. Liang, R. S. Liu, Y. T. Huang, P. T. Wu and L. J. Chen, *Physica* C, 347 (1990) 165.
11. W. H. Lee and D. C. Wang, *Physica* C, 156 (1995) 253.
12. W. Y. Yip and R. Abd-Shukor, *J. Supercond. Nov. Magn*., 705 (2009) 22.
13. Z. Z. Sheng, Y. F. Li and D. O. Pederson, *Solid State Communication*, 80 (1991) 913.
14. I. B. Parise, P. I. Gai, M. A. Subramanian, J. Gopalakrishnan and A. W. Sleight, *Physica* C, 159 (1989) 245.
15. 15 . S. Li, M. Greenblatt, *Physica* C, 365 (1989) 157.
16. R. Abd-Shukor and K. S. Tee, *Materials Science Letters*, 103-106 (1998) 17.
17. Y. F. Li, O. Chmaissem and Z. Z. Sheng , *Physica* C, 248 (1995) 42.
18. M.A. Subramanian, C.C. Torardi, J. Gopalakrishnan, P.L. Gai, J.C. Calabrese, T.R. Askew, R.B.Flippen and A.M. Sleight, *Science*, 242 (1988) 249.
19. R. Abd-Shukor and Nor Azah Nik Jaafar, *J. Mater. Sci., Mater. Electron*., 677 (1999) 10.
20. S. Ismail, A.K. Yahya and N.A. Khan, *Ceramics International*. 39 (2013) S257.
21. S.V. Sharma, G. Sinha, T.K. Nath, S. Chakroborty and A.K. Majumdar, *Physica* C. 242 (1995) 351.
22. T. Sato, H. Nakane, N. Mori and S. Yoshizawa, *Physica* C. 357–360 (2001) 244.
23. A. Ali Yusuf, A.K. Yahya, N.A. Khan, F. Md. Salleh, E. Marsom and N. Huda, *Physica* C. 471 (11-12) (2011) 363.

24. N.H. Ahmad, N.A. Khan and A.K. Yahya, *Journal of Alloys and Compounds*. 492 (1-2) (2010) 473.
25. N. A. Khan and A. Mumtaz, *Physica* B. 404 (13) (2010) 2772.
26. N.A. Khan, N. Hassan, M. Irfan and T. Firdous, *Physica* B. 405 (6) (2010) 1541.
27. Z. Z. Sheng, D. X. Gu, Y. Xin and D. O. Pederson, *Modern Physics Letters* B. 9 (1991) 635.
28. N. Huda, A.K. Yahya and W.F. Abdullah, American Institute of Physics (AIP) Proceedings, American Institute of Physics. 1017 (2008) 114.
29. N.A Khan and M. Irfan, *Physica* C. 468 (2008) 2341.
30. N.A. Khan and G. Husnain, *Physica* C. 436 (1) (2006) 51.
31. N.A. Khan, A.A. Khurram and A. Maqsood, *Physica* C. 398 (3-4) (2003) 114.
32. N. Huda and A.K. Yahya, *Materials Research Innovation*. 13(3) (2009) 406.
33. R. Awad, A.I. Abou-Aly, I.H. Ibrahim and W. Abddeen, *Solid State Communications*. 146(1) (2008) 92.
34. N. Rahman, K. B. Tan, Z. Zainal, C. C. Khaw, M. P. Chon, *Sains Malaysiana* 44(7) (2015) 1003.
35. M. K. Halimah, W. H. Chiew, H. A. A. Sidek, W. M. Daud, Z. A. Wahab, A. M. Khamirul S. M. Iskandar, *Sains Malaysiana* 43(6) (2014) 899.
36. I. Hamadneh. Y. W. Kuan, L.T. Hui, R. Abd-Shukor, *Materials Letters* 60 (2006) 734.
37. A. Al-Sharabi, R. Abd-Shukor, *Journal of Alloys and Compounds* 615 (2014) 363.